Preparation of EMI Shielding and Corrosion-Resistant Composite Based on Electroless Ni-Cu-P Coated Wood

Bin Hui, Jian Li, and Lijuan Wang*

A simple electroless Ni-Cu-P plating process for preparing an EMI-shielding and corrosion-resistant wood-based composite has been developed. The effects of solution pH value on the metal deposition, surface resistivity, chemical composition, anti-corrosion properties, and crystal structure of the coatings were studied. The coatings were characterized using X-ray photoelectron spectroscopy, X-ray diffraction, and scanning electron microscopy. When the solution pH was increased from 8.5 to 10.0, the metal deposition increased and the surface resistivity decreased. Chemical composition indicated that the nickel deposition increased, whereas the opposite effect was obtained on copper and phosphorus elements with a pH increase from 9.0 to 10.0, and the crystal structure of the Ni-Cu-P coatings changed from an amorphous state to a microcrystalline one. Tafel curves of the Ni-Cu-P coatings prepared at pH 9.0 or 9.5 showed that they had excellent anti-corrosion properties in a 3.5 wt% NaCl solution. The morphology of the coating containing 69.86% Ni - 7.65% Cu - 22.49% P is superior to that with 75.99% Ni - 6.60% Cu - 17.41% P after corrosion tests. The plated birch veneers exhibited electromagnetic shielding effectiveness higher than 58 dB in frequencies ranging from 9 KHz to 1.5 GHz, and the coating firmly adhered to the wood surface.

Keywords: Birch veneer; Electroless Ni-Cu-P plating; Electromagnetic shielding effectiveness; Anti-corrosion

Contact information: Key Laboratory of Bio-based Material Science and Technology of Ministry of Education, Northeast Forestry University, 26 Hexing Road, Harbin 150040, P. R. China;
** Corresponding author: donglinwlj@163.com*

INTRODUCTION

Wood is a natural biomass material that has important potential functions and attributes, such as temperature and humidity control, heat and sound insulation, and a high ratio of strength to weight. Wood-based electromagnetic shielding material has attracted much attention recently. Many previous studies focused on electroless plating Ni-P or copper coatings on wood veneers (Nagasawa and Kumagai 1989; Nagasawa *et al.* 1990, 1991a, 1991b, 1992, 1999; Huang and Zhao 2004; Wang *et al.* 2006a, 2006b, 2008, 2011a, 2011b, 2011c; Wang and Li 2007; Sun *et al.* 2012; Sha *et al.* 2011). However, the corrosion resistance of Ni-P or copper coatings is poor.

Studies show that Ni-Cu-P coatings have better anti-corrosion properties than Ni-P or copper coatings. Electroless deposition of Ni-Cu-P alloys and the effects of some parameters on the properties of coatings have been studied by many researchers. Krasteva *et al.* (1994) demonstrated that the introduction of copper into electroless deposited Ni-P alloys conferred higher thermal and nonmagnetic stability. Yu *et al.* (2001) compared the crystallization behavior of electroless Ni-P and Ni-Cu-P coatings using differential

scanning calorimetry and X-ray diffractrometry. Also, Ni-Cu-P deposition results in more corrosion resistance and lower corrosion current density (I_{corr}) than Ni-P deposition under various conditions (Abdel Hameed and Fekry 2010). Ni-Cu-P coatings on substrates such as Al, polyester fabric, and carbon steel have been widely studied (Valova *et al.* 2005; Guo *et al.* 2009; Ranganatha *et al.* 2012); however, there have been no reports concerning the deposition of Ni-Cu-P coatings on wood material.

Nonmetallic materials require activation before electroless plating because there are no catalytic nuclei normally present on their surface to act as initiators. In the conventional activation process, palladium colloid is widely used prior to plating. Palladium colloid is a noble metal, and the cost is very high. Because of this, Pd-free activation systems have been sought. Though significant progress has been made in Pd-free activation during the past several years, the high cost and the need for better stability have prompted researchers to consider novel approaches to activation. Two methods have been widely investigated. One is the reduction of Ni^{2+} on the surface of the substrate to Ni^0 by thermal treatment at higher temperatures (Wang and Wu 2003; Li *et al.* 2006; Shao *et al.* 2007; Li and An 2008; Tang *et al.* 2009); the other is the production of Ni^0 on the substrate from absorbed Ni^{2+} by the use of $NaBH_4$ in two separate steps (Hu *et al.* 2006; Lai *et al.* 2006; Gao and Huang 2007). Wood is naturally porous and hydrophilic, with plenty of hydroxyl groups. In our previous studies, a novel and simple activation method was used for nickel or copper plating on wood veneers (Li *et al.* 2010; Wang *et al.* 2011a). With a simple and low-cost method, the technology is utilized in the synthesis of Ni-Cu-P coatings. In this study, the effect of solution pH on the metal deposition, conductivity, chemical composition, and crystal structure was examined. Tafel curves were studied to evaluate the anti-corrosion ability of the material's surface using an electrochemical work station. The coating on the wood veneer was characterized by scanning electron microscopy (SEM), X-ray diffraction (XRD), and X-ray photoelectron spectroscopy (XPS).

EXPERIMENTAL

Materials

The substrates used in the experiments were birch wood veneers with 0.6 mm thickness. The veneers were polished with emery papers to remove fine fibers or dust on the surface. The samples for electric conductivity studies were cut into squares 50 mm × 50 mm in size. The samples for corrosion studies were cut into squares 30 mm × 30 mm in size. Sodium hypophosphite was obtained from Tianjin Kermel Chemical Reagent. All other chemicals were of analytical grade.

Activation and Plating

The procedure for preparation of the EMI-shielding and corrosion-resistant wood-based composite is shown in Fig. 1. Wood veneers were immersed into $NaBH_4$ solution containing 5 g/L sodium hydroxide for a time sufficient to load enough $NaBH_4$ on the surface. Then, the veneer of loading $NaBH_4$ and NaOH was put in a plating bath to achieve the activation and electroless plating in one bath. The samples were plated for a special time, removed from the bath, washed with tap water, and air-dried to constant weight. The composition of electroless solution and operation conditions are listed in Table 1, and the solution pH was adjusted with $NH_3 \cdot H_2O$.

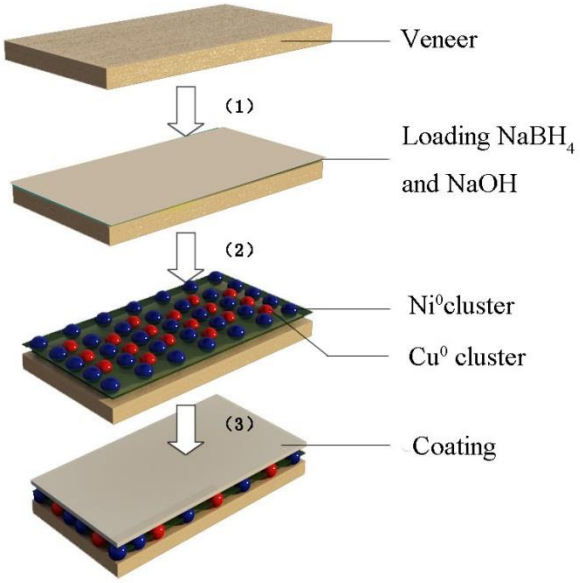

Fig. 1. Schematic illustration of electroless Ni-Cu-P plating process

The reducing ability of $NaBH_4$ is superior to that of $H_2PO_2^-$. So, Ni^{2+} of plating solution firstly reacted with $NaBH_4$, which produced Ni^0 clusters as the catalytic center, initiating subsequent electroless plating. However, Cu^{2+} can be reduced by $NaBH_4$, generating Cu^0 clusters. Because of the copper overlapping the partial catalytic center, controlling the $CuSO_4$ concentration is vital. Activating stages are described by the following equations:

$$2Ni^{2+} + BH_4^- + 2H_2O \rightarrow 2Ni^0 + 2H_2\uparrow + BO_2^- + 4H^+ \quad (1)$$

$$[2Cu^{2+} + BH_4^- + 2H_2O \rightarrow 2Cu^0 + 2H_2\uparrow + BO_2^- + 4H^+] \quad (2)$$

Table 1. Composition and Operation Conditions of Electroless Ni-Cu-P Plating

Chemical	Content ($g \cdot L^{-1}$)
$NiSO_4 \cdot 6H_2O$	30
$CuSO_4 \cdot 5H_2O$	1.0
$NaH_2PO_2 \cdot H_2O$	40
Sodium citrate	50
Buffering agent	35
pH	8~11
T	90 °C

Measurement of Metal Deposition

The wood veneers were dried at 103±2 °C to constant weight (G_0). Ni-Cu-P-coated veneers were also dried to constant weight (G_1), and the metal deposition was calculated as follows:

$$\text{Metal deposition}\ (\%) = (G_1 - G_0) / G_0 \times 100\% \quad (3)$$

Surface Resistivity and Shielding Effectiveness

The surface resistivity of the metalized wood veneers was measured using a YD2511A-type smart low direct-current (DC) resistance tester, according to the Chinese National Military Standard GJB2604-96. The calculations were reported previously (Li *et al.* 2010).

The shielding effectiveness (SE) of the metalized wood veneers was measured with an Agilent E4402B spectrum analyzer and standard butt coaxial cable line with flange based on the Chinese industrial standard SJ20524-95. The *SE* value was calculated as,

$$SE\ (\text{dB}) = -10 \times \lg\left(\frac{P_{out}}{P_{in}}\right) \quad (4)$$

where P_{out} and P_{in} are the incident and transmitted power, respectively.

Electrochemical Corrosion Studies

The corrosion tests were carried out using an LK2005A electrochemical work station installed with the usual software. A conventional three-electrode system was utilized in the measurements, where the plated birch veneer was used as the working electrode, with saturated calomel electrode (SCE) as the reference electrode and platinum foil as the counter electrode.

A limited area of 1 cm^2 on the samples was exposed to a 3.5wt% NaCl solution. Prior to the test, each specimen was allowed to stabilize the open-circuit potential (OCP) in the 3.5wt% NaCl solution. Tafel curves were obtained by scanning from -750 mV, below the OCP, to -200 mV at a scanning rate of 1 mV/s.

The corrosion potentials (E_{corr}) and corrosion current densities (I_{corr}) were determined by extrapolating the straight-line section of the anodic and cathodic branches of the Tafel plots.

Surface Analysis

The surface morphology was determined by scanning electron microscopy (SEM, Quanta 200). Specimens were not sprayed with gold prior to analysis. XPS was used for the chemical composition and chemical state analysis of Ni-Cu-P coatings. XPS signals were recorded with a K-Alpha XPS Analyzer (ThermoFisher Scientific Company) using an Al K_α source.

In addition, the crystal structure of the coating was investigated by X-ray diffraction (XRD, Rigaku D/max2200 diffractometer) using a Cu K_α radiation generator operated at 1200 W (40 kV×30 mA).

Bonding Strength Measurement

A vertical pulling method was employed to measure the adhesion between the Ni-Cu-P coating and the substrate. A loading fixture was attached to the surface of the specimen to be tested using a melt adhesive, and a circle around the loading fixture was

cut from the coating. The adhesion was then measured with a universal testing machine (Shimadzu AG-10TA).

RESULTS AND DISCUSSION

Effects of Solution pH on Metal Deposition and Surface Resistivity

The pH is a key factor for electroless plating Ni-Cu-P alloys. The effects of pH value on the metal deposition and surface resistivity are shown in Fig. 2. The metal deposition increased from 29.52% to 44.14% with an increase in pH from 8.5 to 9.5. The surface resistivity was negatively correlated with metal deposition. The surface resistivity sharply decreased from 981.6 mΩ/cm^2 to 408.1 mΩ /cm^2. Further increasing the pH was not able to markedly change the metal deposition and surface resistivity. The minimum surface resistivity was 377.4 mΩ/cm^2, which is higher than the roughly 240 mΩ/cm^2 of Ni-P coating and the 120 mΩ/cm^2 of copper coating on birch wood veneers (Liu *et al.* 2010; Sun *et al.* 2012).

The content of phosphorus can affect the conductive properties. According to equations (5) and (7) below, the increase in solution pH can accelerate the reaction to produce more nickel and repress the phosphorus content. In fact, if pH increased continuingly, the plating solution would decompose because of excess OH^- combined with Ni^{2+} and Cu^{2+}, producing $Ni(OH)_2$ and $Cu(OH)_2$. The autocatalytic stage is expressed by the following three equations (5, 6, and 7):

$$2H_2PO_2^- + 4OH^- + Ni^{2+} \rightarrow 2HPO_3^{2-} + 2H_2O + Ni\downarrow + H_2\uparrow \quad (5)$$

$$2H_2PO_2^- + 4OH^- + Cu^{2+} \rightarrow 2HPO_3^{2-} + 2H_2O + Cu\downarrow + H_2\uparrow \quad (6)$$

$$2H_2PO_2^- + 6H^+ + 4H^- \rightarrow 4H_2O + 2P\downarrow + 3H_2\uparrow \quad (7)$$

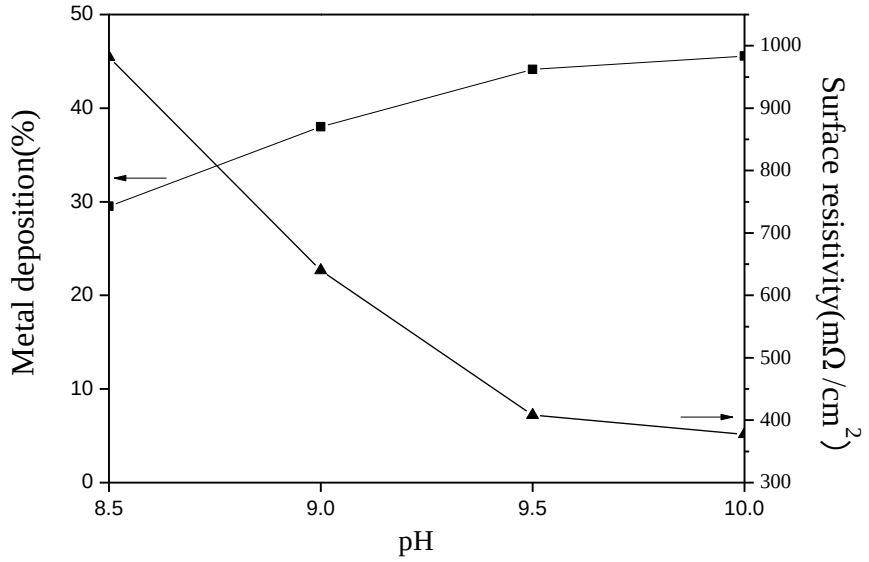

Fig. 2. Effect of solution pH on metal deposition and surface resistivity

Chemical Composition and Crystal Structure

The pH plays an important role in the chemical composition and crystal structure of plating alloys. Figure 3 shows the chemical composition of Ni-Cu-P coatings in the pH range from 9.0 to 10.0, and the corresponding crystal structure is showed in Fig. 4.

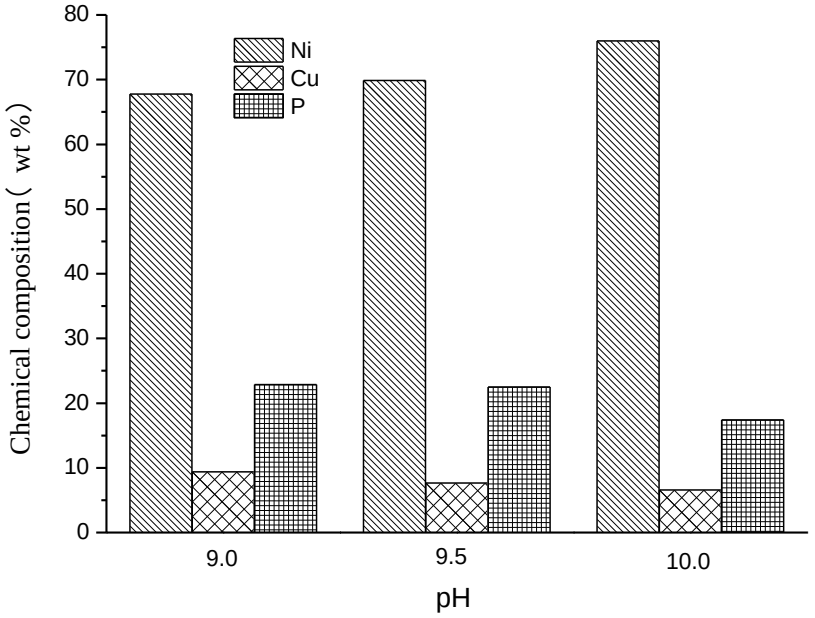

Fig. 3. Deposition composition of the coatings

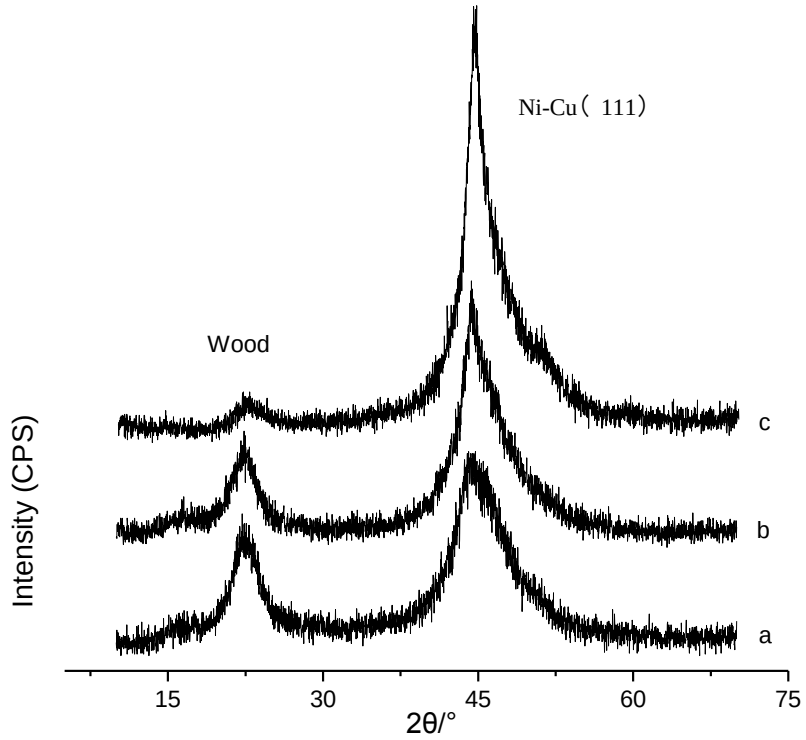

Fig. 4. XRD patterns of the coatings prepared from the baths (a) pH=9.0; (b) pH=9.5; (c) pH=10.0

By increasing the solution pH from 9.0 to 10.0, the deposition of nickel increased, whereas the opposite effect was obtained with the deposition of copper and phosphorus. XRD analysis showed a peak in the curve at 2θ=22.18°, which is a characteristic peak of cellulose in birch veneer. In addition, the peaks become smaller as the pH increases from 9.0 to 10.0. The peak at 2θ=44.52° is attributed to Ni-Cu(111), which indicated the structure is amorphous or microcrystalline. However, it is obvious that the crystal structure of the Ni-Cu-P coatings changes from an amorphous to microcrystalline state with an increase in solution pH. The changes in nickel and phosphorus can be explained by the equations 5 and 7. Copper content was lower with increasing solution pH, which is attributed to the fact that the ability of citrate coordinated to copper ions is greatly enhanced in alkaline conditions, compared with that of nickel ions. The crystal structure of Ni-Cu-P coatings can be ascribed to the phosphorus content. The lower phosphorus content is in a crystalline or microcrystalline state, and it reaches an amorphous state as the phosphorus content becomes higher. The reason why the cellulose peaks became weaker is that the coatings grew increasingly thick as the pH increased from 9.0 to 10.0, conforming to Fig. 2.

Corrosion Studies

Figure 5 shows Tafel plots registered for the coatings in a 3.5 wt% NaCl solution. The corrosion potential (E_{corr}) and corrosion current density (I_{corr}) are shown in Table 2.

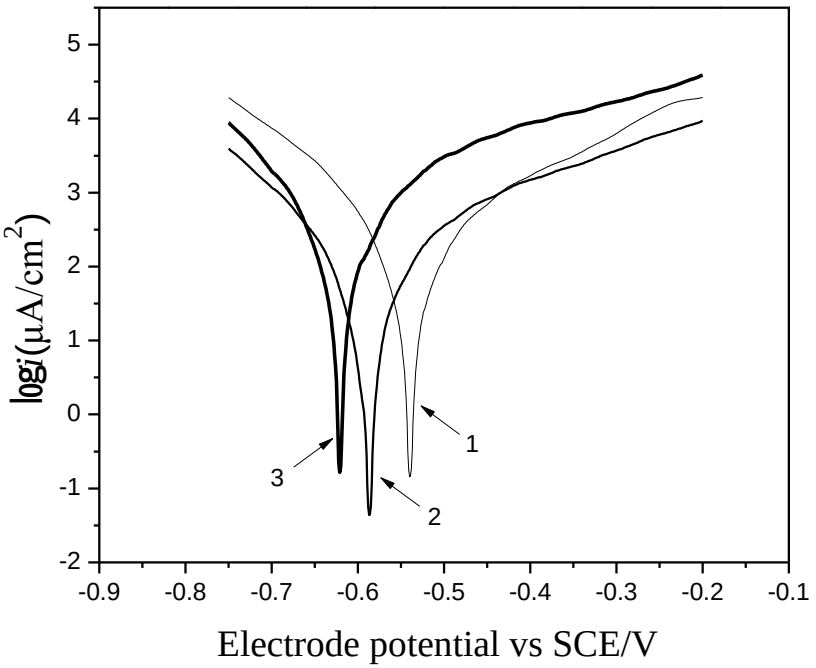

Fig. 5. Tafel plots tested in a 3.5 wt% NaCl solution for Ni-Cu-P coatings prepared from the baths (1) pH=9.0; (2) pH=9.5; (3) pH=10.0

With a pH increase from 9.0 to 10.0, the Tafel plots of Ni-Cu-P coatings showed a negative potential shift, in which the current density first decreased and then increased. From the perspective of thermodynamics, the more positive the potential, the stronger the corrosion resistance tends to be. On the other hand, a low current density shows good

anti-corrosion ability. The anti-corrosion ability of the coatings prepared at pH 9.0 or 9.5 was better than the coating prepared at pH 10.0. This can be attributed to the content of copper and phosphorus. The higher the copper and phosphorus contents are, the better the anti-corrosion ability is. Further, the incorporation of Cu can reduce the free energy of Ni-Cu-P alloy due to the higher thermodynamic stability of Cu than that of Ni. The phosphorus element is very stable under various conditions. According to Fig. 3, the copper and phosphorus content of the coating prepared at solution pH 10.0 was 24.01%, which was lower than that of coatings prepared at pH 9.0 or 9.5.

Table 2. Corrosion Characteristics of Electroless Ni-Cu-P Plating

Sample	Scanning Range (V)	E_{corr} (V vs. SCE)	I_{corr} (A/cm^2)
1	-0.75 ~ -0.2	-0.539	1.48×10^{-7}
2	-0.75 ~ -0.2	-0.587	4.37×10^{-8}
3	-0.75 ~ -0.2	-0.621	1.66×10^{-7}

Surface Morphology

The two specimens measured were respectively prepared at solution pH values of 9.5 and 10.0. The surface morphology of the latter exhibited a coarse nodular structure, as shown in Fig. 7.

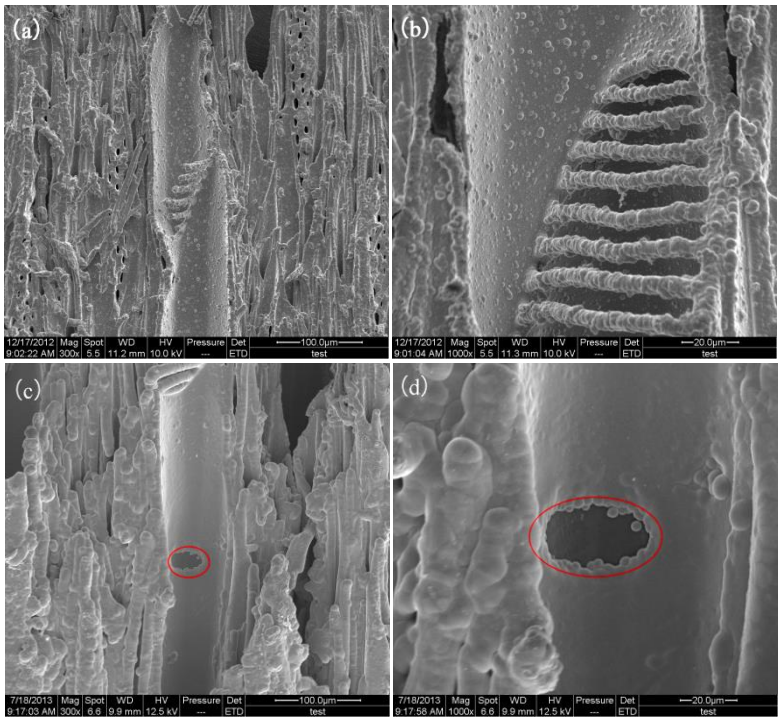

Fig. 6. SEM images of plated Ni-7.65%Cu-22.49%P on wood veneer before (a and b) and after (c and d) corrosion tests

Copper is an important factor in repressing the activation of additional nodular sites and leads to low coating porosity. With increasing copper content of plated layers, the nodular characteristics of deposited particles were increasingly inconspicuous, the diameter of deposited particles became small, and the gap between deposited particles

was also diminished, which rendered the surface structure more compact (Fig. 6). After corrosion tests in a 3.5 wt% NaCl solution, the images of plated Ni-7.65%Cu-22.5%P on wood veneer (Fig. 6, c, and d) were superior to that of plated Ni-6.60%Cu-17.41%P veneer (Fig. 7, g, and h). This is in accordance with the results of corrosion studies and can be attributed to the content of copper and phosphorus.

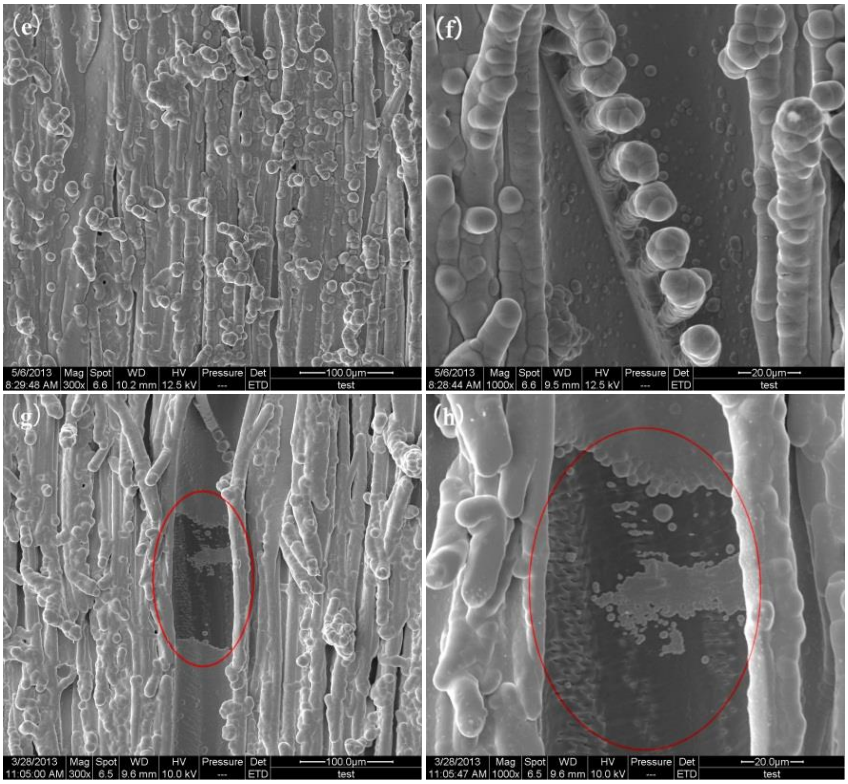

Fig. 7. SEM images of plated Ni-6.60%Cu-17.41%P on wood veneer before (e and f) and after (g and h) corrosion tests

XPS Analysis

XPS measurements were utilized to obtain more information about the chemical state of the Ni-Cu-P coating obtained at solution pH 9.5. A typical XPS wide spectrum of the surface of the plated veneer is shown in Fig. 8, which reveals that nickel, copper, and phosphorus elements with some Ni^{2+}, C, and O were detected. The peaks at 932.14 eV, 129.23 eV, 531.36 eV, and 284.68 eV are attributed to Cu2p, P2p, O1s, and C1s, respectively (Wang *et al.* 2011; Liu *et al.* 2012).

To further determine the inner composition of the plated coating, it was etched by an argon ion sputter for 30 s to eliminate contaminants from the surface. The peaks of C and O disappeared, which indicates that the contaminants were the source of solution absorbed by the plated veneer.

In the XPS high-resolution scan of Ni2p, it was found that the elementary composition of the surface contained Ni^0, Ni^{2+}, and $Ni(OH)_2$ (Fig. 9a), whereas the only Ni^0 with some $Ni(OH)_2$ (Fig. 9b) existed in the inner part of the plated layer, which showed that Ni^{2+} had been reduced to Ni^0 in the plating process (Liu *et al.* 2012). $Ni(OH)_2$ was mainly produced by Ni^{2+} reacting with excess OH^-.

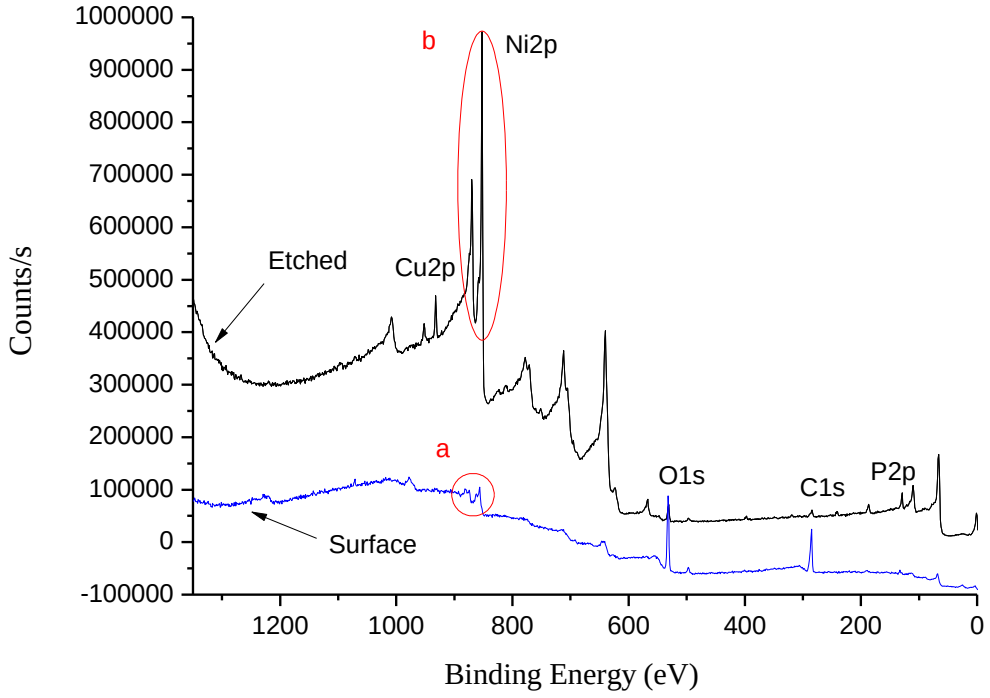

Fig. 8. XPS spectra of Ni-Cu-P coating on birch veneer

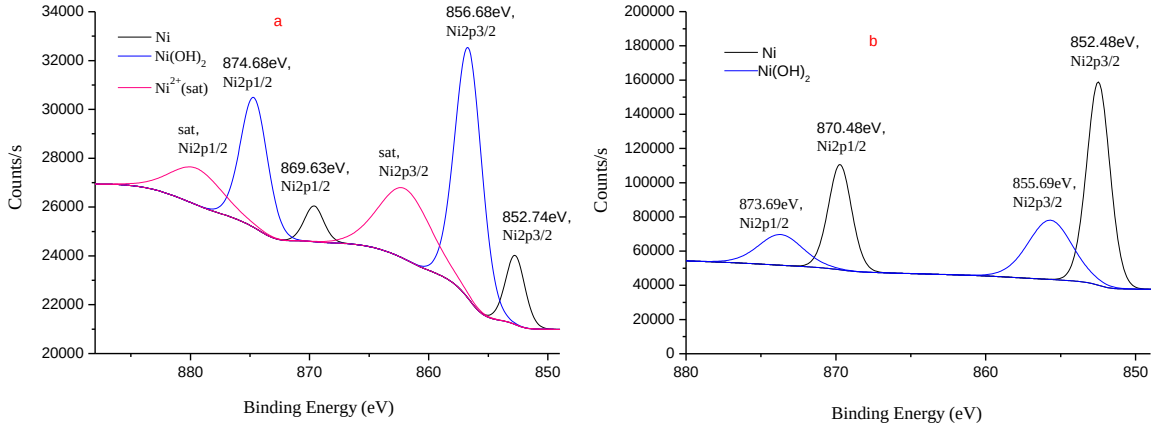

Fig. 9. High-resolution XPS spectra of Ni on the coating surface before (a) and after (b) etching

Shielding Effectiveness

Figure 10 shows electromagnetic shielding effectiveness (SE) of the raw veneer and Ni-Cu-P plated veneers with different pH value in the plating bath. The raw birch veneer had almost no shielding effectiveness, as shown in Fig. 10a. With increasing pH from 9.0 to 10.0, the electromagnetic shielding results of plated wood veneers were higher in frequencies from 9 KHz to 1.5 GHz, as shown in Fig. 10, b, c, and d. According to Schelkunoff's theory, better conductivity of Ni-Cu-P-coated veneers leads to a higher level of SE. It is seen in Fig. 2 that the surface resistance decreased with higher pH value.

Further, The SE value of the sample at pH 10.0 exceeded 58 dB in all frequencies. It is regarded as an effective shield if the SE value exceeds 35 dB. Therefore, the plated wood can become a promising lightweight anti-EMI composite.

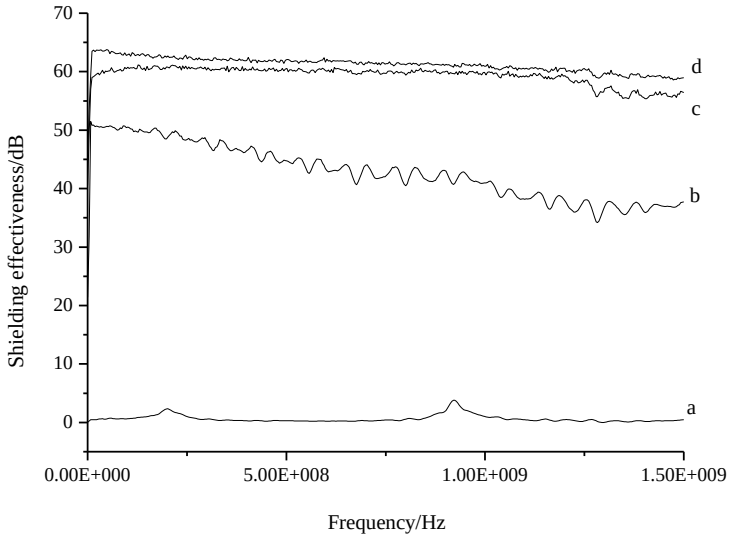

Fig. 10. Shielding effectiveness of Ni-Cu-P-coated veneers prepared from the baths (a) pristine veneer; (b) pH=9.0; (c) pH=9.5; (d) pH=10.0

Adhesion of Ni-Cu-P Coatings to Wood

The test results for adhesion between the coating and the wood surface are shown in Table 3. The five specimens measured were obtained under the optimum condition of solution pH 9.5. It is clearly seen that the formed samples were damaged in the adhesive layer. Therefore, the data listed in Table 3 cannot be really equal to the bonding strength between the coating and wood surface; they can only reflect the strength of the adhesive layer. The experimental phenomena make it clear that the coating firmly bonded to the surface of wood. The reason for its high strength is that wood is naturally porous and has irregularities suitable for mechanical anchorage. In short, the adhesion strength can meet the needs of common applications.

Table 3. Test Results for Adhesion between the Coating and Wood Surface

Specimen	Bonding strength/MPa	Rupture phenomenon observed
1	3.872	Adhesive-layer rupture
2	3.475	Adhesive-layer rupture
3	4.387	Adhesive-layer rupture
4	4.115	Adhesive-layer rupture
5	2.894	Adhesive-layer rupture

CONCLUSIONS

1. Electroless plating Ni-Cu-P alloys were successfully achieved on birch veneer in a simple process.

2. The plating solution pH value had a significant effect on the performance of the plated veneer. The metal deposition increased and the surface resistivity sharply decreased with a pH increase from 8.5 to 9.5, while further increasing pH did not significantly change the metal deposition and surface resistivity.
3. With a pH increase from 9.0 to 10.0, nickel increased, copper and phosphorus decreased, and the crystal structure of the Ni-Cu-P coatings changed from an amorphous to a microcrystalline state.
4. Tafel curves showed the Ni-Cu-P coating prepared in solutions with pH 9.0 or 9.5 had better anti-corrosion properties in a 3.5 wt% NaCl solution.
5. The images of plated 69.86% Ni - 7.65 % Cu - 22.49% P on wood veneer were superior to that of plated 75.99% Ni - 6.60% Cu - 17.41% P veneer after corrosion tests in a 3.5 wt% NaCl solution.
6. XPS analysis indicated the birch veneer was coated with Ni-Cu-P alloys, and the coating was firmly bonded to the wood surface.
7. EMI shielding results for the wood-based Ni-Cu-P composite prepared at solution pH 10.0 were higher than 58 dB in frequencies from 9 KHz to 1.5 GHz.

ACKNOWLEDGMENTS

The authors gratefully acknowledge the Forestry Industry Research Special Funds for Public Welfare Projects (No. 201304502).

REFERENCES CITED

Abdel Hameed, R. M., and Fekry, A. M. (2010). "Electrochemical impedance studies of modified Ni-P and Ni-Cu-P deposits in alkaline medium," *Electrochimica Acta* 55(20), 5922-5929.

Gao, G. Q., and Huang, J. T. (2007). "The effect factor analysis of the nickel activation techniques on the uniformity of the plating layer in wood electroless nickel plating," *Journal of Inner Mongolia Agricultural University* 28, 95-98.

Guo, R. H., Jiang, S. Q., Yuen, C. W. M., and Ng, M. C. F. (2009). "Effect of copper content on the properties of Ni-Cu-P plated polyester fabric," *Journal of Applied Electrochemistry* 39(6), 907-912.

Hu, G. H., Wu, H. H., and Yang, F. Z. (2006). "Electroless nickel plating on carbon nanotube with non-palladium activation process," *Electrochemistry* 12(1), 25-28.

Huang, J. T., and Zhao, G. J. (2004). "Electroless plating of wood," *Journal of Beijing Forestry University* 3, 88-92.

Krasteva, N., Fotty, V., and Armyanov, S. (1994). "Thermal stability of Ni-P and Ni-Cu-P amorphous alloys," *Journal of the Electrochemical Society* 141(10), 2864-2867.

Lai, D. Z., Chen, W. X., Yao, Y. F., and Liu, G. F. (2006). "Novel activation method using chemical plating on the fabric," *Journal of Textile Research* 27(1), 34-37.

Li, J., Wang, L. J., and Liu, H. B. (2010). "A new process for preparing conducting wood veneers by electroless nickel plating," *Surface and Coatings Technology* 204(8), 1200-1205.

Li, L. B., An, M. Z., and Wu, G. H. (2006). "A new electroless nickel deposition technique to metallise SiCp/Al composites," *Surface and Coatings Technology* 200(16), 5102-5112.

Li, L. B., and An, M. Z. (2008). "Electroless nickel-phosphorus plating on SiCp/Al composite from acid bath with nickel activation," *Journal of Alloys and Compounds* 461(1), 85-91.

Lin, W. S, and Huang, W. H. (2003). "Electroless nickel plating on glass substrate by palladium-free activation," *Chinese Journal of Applied Chemistry* 20(5), 018.

Liu, H., Guo, R. X., Liu, Y., Thompson, G. E., and Liu, Z. (2012). "The effect of processing gas on corrosion performance of electroless Ni-W-P coatings treated by laser," *Surface and Coatings Technology* 206(15), 3350-3359.

Liu, H., Li, J., and Wang, L. J. (2010). "Electroless nickel plating on APTHS modified wood veneer for EMI shielding," *Applied Surface Science* 257(4), 1325-1330.

Nagasawa, C., and Kumagai, Y. (1989). "Electromagnetic shielding particleboards with nickel-plated wood particle," *Journal of Wood Science* 35(12), 1092-1099.

Nagasawa, C., Kumagai, Y., and Urabe, K. (1990). "Electromagnetic shielding effectiveness of particleboard containing nickel-metalized wood-particles in the core layer," *Journal of Wood Science* 36(7), 531-537.

Nagasawa, C., Kumagai, Y., and Urabe, K. (1991a). "Electroconductivity and electromagnetic-shielding effectiveness of nickel-plated veneer," *Journal of Wood Science* 37(2), 158-163.

Nagasawa, C., Kumagai, Y., Koshizaki, N., and Kanbe, T. (1992). "Changes in electromagnetic shielding properties of particleboards made of nickel-plated wood particles formed by various pre-treatment processes," *Journal of Wood Science* 38(3), 256-263.

Nagasawa, C., Kumagai, Y., Urabe, K., and Shinagawa, S. (1999). "Electromagnetic shielding particle board with nickel-plated wood particles," *Journal of Porous Materials* 6(3), 247-254.

Nagasawa, C., Umehara, H., and Koshizaki, N. (1991b). "Effects of wood species on electroconductivity and electromagnetic shielding properties of electrolessly plated sliced veneer with nickel," *Journal of Wood Science* 40(10), 1092-1099.

Ranganatha, S., Venkatesha, T. V., and Vathsala, K. (2012). "Process and properties of electroless Ni-Cu-P-ZrO_2 nanocomposite coatings," *Materials Research Bulletin* 47(3), 635-645.

Sha, W., Wu, X., and Keong, K. G. (2011). *Electroless Copper and Nickel-Phosphorus Plating: Processing, Characterisation and Modeling*, Woodhead Publishing, Cambridge, UK.

Shao, Q., Yang, Y. X., Ge, S. S., and Zheng, H. (2007). "Study on electroless nickel plating activated without palladium on the surface of cenospheres," *Journal of Functional Materials* 38(12), 2001.

Sun, L., Li, J., and Wang, L. J. (2012). "Electromagnetic interference shielding material from electroless copper plating on birch veneer," *Wood Science and Technology* 46(6), 1061-1071.

Valova, E., Dille, J., Armyanov, S., Georgieva, J., Tatchev, D., Marinov, M., Delphancke J.-L., Steenhaut ,O., and Hubin, A. (2005). "Interface between electroless amorphous Ni-Cu-P coatings and Al substrate," *Surface and Coatings Technology* 190(2), 336-344.

Wang, L. J, Sun, L., and Li, J. (2011b). "Electroless copper plating on *Fraxinus mandshurica* veneer using glyoxylic acid as reducing agent," *BioResources* 6(3), 3493-3504.

Wang, L. J., and Li, J. (2007). " Ultrasound-assisted electroless plating Ni-P alloy on the surface of birch veneer," *Scientia Silvae Sinicae* 12, 311-315.

Wang, L. J., and Liu, H. B. (2011c). "Electroless nickel plating on chitosan-modified wood veneer," *BioResources* 6(2), 2045-2054.

Wang, L. J., Li, J., and Liu, H. B. (2011a). "A simple process for electroless plating nickel-phosphorus film on wood veneer," *Wood Science and Technology* 45(1), 161-167.

Wang, L. J., Li, J., and Liu, Y. X. (2006a). "Electroless nickel plating on poplar veneer," *Fine Chemicals* 23(3), 230-233.

Wang, L. J., Li, J., and Liu, Y. X. (2006b). "Preparation of electromagnetic shielding wood-metal composite by electroless nickel plating," *Journal of Forestry Research* 17(1), 53-56.

Wang, L. J., Li, J., and Liu, Y. X. (2008). "Study on preparation of electromagnetic shielding composite by electroless copper plating on *Fraxinus mandshurica* veneer," *Journal of Material Engineering* (4), 56-60.

Yu, H. S., Luo, S. F., and Wang, Y. R. (2001). "A comparative study on the crystallization behavior of electroless Ni-P and Ni-Cu- P deposits," *Surface and Coatings Technology* 148(2), 143-148.

Article submitted: July 24, 2013; Peer review completed: October 1, 2013; Revised version received and accepted: October 5, 2013; Published: October 8, 2013.